

# Are Chaplygin gases serious contenders to the dark energy throne?

Rachel Bean and Olivier Dore

Department of Astrophysical Sciences, Princeton University,  
Princeton Hall – Ivy Lane, Princeton, NJ08544-1001, USA  
rbean@astro.princeton.edu, olivier@astro.princeton.edu

(Dated: February 7, 2020)

We study the implications on both background and perturbation evolution of introducing a Chaplygin gas component in the universe's ingredients. We perform likelihood analyses using wide-ranging, SN 1a, CMB and large scale structure observations to assess whether such a component could be a genuine alternative to a cosmological constant. We find that current data favors a cosmological constant thus not motivating further studies of such a component.

## I. INTRODUCTION

Supernovae observations [1, 2] first indicated that the universe's expansion has started to accelerate during recent cosmological times. This, and further observations, e.g. of the Cosmological Microwave Background (CMB) or Large Scale Structures (LSS), suggest that the energy density of the universe is dominated by a dark energy component, with a negative pressure, driving the acceleration. One of the substantive goals for cosmology, and for fundamental physics, is ascertaining the nature of this dark energy. Maybe the most attractive option would be a cosmological constant, , however there are infamous fine-tuning and coincidence problems associated with explaining why should have today's energy scale. These problems have led to a wealth of dynamical, scalar, dark energy ("quintessence") models being proposed as alternatives to (see [3] for a good review). Even in these cases, however, explaining why our epoch should be so crucial in triggering the acceleration still requires fine-tuning.

A concurrent problem is the nature of the non-baryonic, clumping dark matter component required in the standard model to give Large Scale Structure predictions consistent with observations.

Recently an alternative matter candidate, a Generalized Chaplygin Gas (GCG), has been proposed as a potential 'hybrid' solution to both the dark energy and dark matter problems. A recent letter [4] dealt with the implications for the matter power spectrum in the absence of CDM and effectively ruled out the GCG as a CDM substitute.

In this paper we investigate the strength of the GCG as a dark energy candidate. Although there have been a number of papers discussing various aspects of GCG behavior ([5]–[9]) there has not been, as yet, a full analysis of the constraints that can be placed on such models from the wide range of complementary data sets currently available. This is necessary if such exotic matter types are to be considered as serious alternatives to the -CDM scenario.

In section II we review the background evolution of the GCG and discuss the implications for supernovae (SN 1a) observations. Although such constraints are important, a

wide range of proposed theories can generate the required expansion profile (see [3] for dark energy theories and, for example, [10] for an alternative to dark energy). In order to better discriminate between theories, perturbation dependent observables must be taken into consideration. In section III we extend our discussion to perturbations in the Chaplygin gas and discuss the implications for structure formation. In section IV we consider the effects on radiation perturbations and the CMB spectrum. In section V we present the main results of the paper, likelihood analyses for a CDM + GCG + baryon universe. We obtain a clear indication of the strength of the GCG model when compared to . In section VI we summarize our findings and assess the true potential of Chaplygin gases as a dark energy contender.

## II. BACKGROUND EVOLUTION

The Generalized Chaplygin models can be characterized by three parameters:  $w_0$ , and  $\frac{w_0}{\chi}$ . The equation of state nowadays  $w(a = 1) = \frac{w_0}{\chi}$  and the index specifies the equation of state evolution,

$$p = \frac{w_0 \rho}{\chi} : \quad (1)$$

The energy conservation equation,  $-\dot{\chi} + 3H(1+w) = 0$ , admits a solution for (a) specified by  $\frac{w_0}{\chi}$  and the fractional energy density today,  $\frac{w_0}{\chi}$ ,

$$(a) = \frac{w_0}{\chi} \frac{1}{\chi} \frac{1}{1+w} \frac{1}{a^{3(1+w)}} \quad (2)$$

where  $\chi_0 = 3H_0^2/8G = 1$  is the total energy density today. The equation of state then evolves as,

$$w(a) = \frac{\frac{w_0}{\chi}}{\frac{w_0}{\chi} + \frac{1}{a^{3(1+w)}}} : \quad (3)$$

At early times the GCG's equation of state tends to zero, mimicing CDM. The value of determines the redshift of transition between the two asymptotic behaviors; the greater the value of the lower the transition redshift.

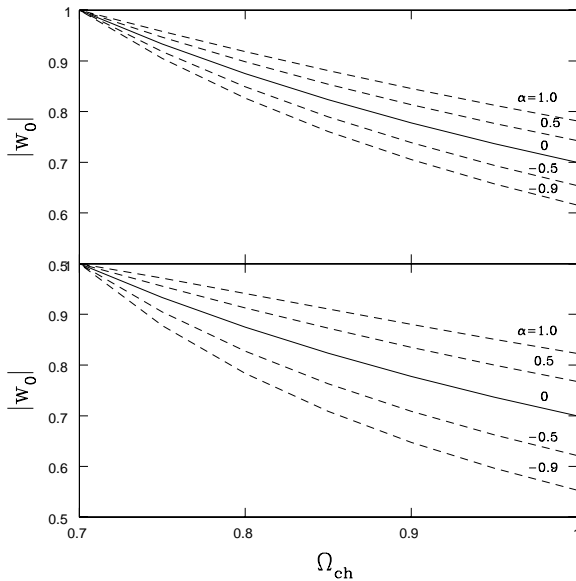


FIG. 1: Contours in  $\Omega_{\text{ch}}$ - $jw_0$  jspace with the same luminosity distance as a *fiducial* model -CDM model with  $\Omega_m = 0.7$  at  $z = 0.5$  (top) and  $z = 1$  (bottom). For  $\alpha = 0$  (full line) the luminosity distance curve is identical to that of the *fiducial* model at all redshifts.

At early times, the total amount of matter with  $w = 0$  reaches an asymptotic value

$$\Omega_m^{\text{eff}} = \Omega_m^0 + \Omega_{\text{ch}}^0 (1 - jw_0)^{\frac{1}{1+w}}$$
 (4)

where  $\Omega_m$  is the baryonic + CDM density fraction. Note that the unique ability of the GCG to account for both the dark energy like behavior at late times and for ordinary dark matter at early times motivated the original studies of this particular equation of state.

In previous discussions has often been assigned a positive value in the range  $0 < w < 1$ , in order to be consistent with various higher dimensional theories that can produce a perfect uid stress-energy tensor satisfying the criterion in (1) (see for example [11]). In our study, we extend the range of values of considered to

$1 < w < 1$  in order to obtain a broader assessment of whether Chaplygin gases could be a viable alternative to the standard model.

For  $w = 0$  the background evolution of the Chaplygin gas is identical to a -CDM model with  $\Omega_{\text{eff}} = \Omega_{\text{ch}}^0 jw_0$  and  $\Omega_m^{\text{eff}} = \Omega_m^0 + \Omega_{\text{ch}}^0 (1 - jw_0)$ . Furthermore, as is visible in equations (2) and (3), when  $jw_0$  tends to 1, the GCG component tends to evolve as a cosmological constant, irrespective of the value of  $w$ . Note that there is no analogous quintessence like behavior (with  $w_0 \neq -1$ ), thus we are only comparing GCG to theories including

The SN 1a observations measure the apparent magnitude,  $m(z)$ , related to the luminosity distance,  $d_L(z)$  via,

$$m(z) = M + 5 \log d_L(z) + 25; \quad (5)$$

$$d_L = (1 + z) \int_0^z \frac{dz^0}{H(z^0)} \quad (6)$$

where  $M$  is the absolute bolometric magnitude and  $d_L$  is measured in M pc. It is easy to see that, because the background evolution (through  $H$ ) wholly determines luminosity distance predictions, the degeneracy between a GCG with  $w = 0$  and -CDM will allow the Chaplygin gas to fit the SN 1a data well. Indeed the degeneracy also stretches to  $w \neq 0$  when one considers luminosity distance at a specific redshift. In figure 1 we show Chaplygin models with degenerate luminosity distances with a *fiducial* -CDM model with  $w = 0.7$ , at  $z = 0.5$  and  $1.0$ . This degeneracy, however, implies that the SN 1a observations cannot be a strong discriminant between the GCG and ; we must look to alternative, perturbation-dependent observations to test the validity of the GCG models.

### III. CHAPLYGIN GAS PERTURBATIONS

We treat the Chaplygin gas as a perfect uid made up of effectively massless particles interacting with the rest of matter purely through gravity. We assume purely adiabatic contributions to the perturbations so that the speed of sound for the uid is

$$c_s^2 = \frac{P}{\rho} = \frac{P}{w} \quad (7)$$

and the time variation of  $w$  is

$$\dot{w} = -3H(1+w)c_s^2 \quad \ddot{w} = 3H\dot{w}(1+w)(+1) \quad (8)$$

where derivatives are with respect to conformal time ( $d/d\eta$ ), and  $aH = da/d\eta$ .

In the synchronous gauge and following the approach and notations of Ma and Bertschinger [12], we can write down the evolution equations for the density and velocity divergence perturbations, and , using the conservation of energy momentum tensor  $T_{\mu\nu} ; = 0$ ,

$$- = (1+w) + \frac{h}{2} - 3H c_s^2 \dot{w} ; \quad (9)$$

$$- = H \dot{1} - 3\dot{c}_s^2 + \frac{c_s^2}{(1+w)} k^2 - k^2 : \quad (10)$$

The uid is highly non-relativistic and therefore we assume the shear perturbation  $\zeta = 0$ .

At early times, when the Chaplygin gas has  $w = 0$ , the GCG perturbations evolve like those of ordinary dust with  $\zeta = 0$ , and  $\zeta = h/2$ . In the radiation era ( $a \propto t^2$ ), while  $\zeta \propto a$  in the early GCG dominated era. At later times, when the GCG's equation of state starts to decrease, the perturbations stray drastically from this dust-like evolution.

We can understand the late-time behavior more clearly if we evaluate the second order differential equation for . By differentiating equation (9) with respect to time

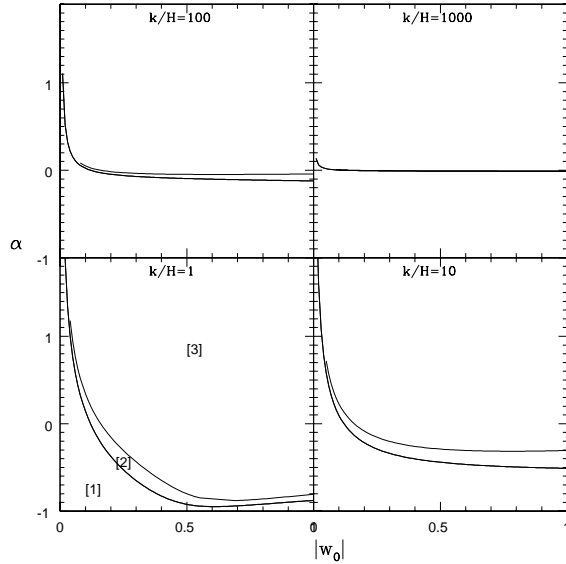


FIG. 2: Late-time evolution as a function of  $|w_0|$  and  $jw_0j$  for 4 scales  $k=H = 1, 10, 100, 1000$  ( $H = 3000hMpc^{-1}$ ;  $h = 0.65$ ). Regions [1] and [2] undergo power law growth and decay respectively and [3] undergoes oscillatory decay.

we find, as outlined in an appendix (section V II), for a general shearless, uid,

$$\begin{aligned}
 & + 1 + 6(c_s^2 - w)H - \\
 & + 9H^2(c_s^2 - w)^2 + 3H(c_s^2 - w) + \frac{a}{a}(c_s^2 - w) + \zeta_s^2 k^2 \\
 & = 3\zeta_s^2(1 + w)H + \frac{a^2}{2}(1 + w)(3P + \dots); \quad (11)
 \end{aligned}$$

Numerical integration shows that the coupling to  $w$  in equation (11) is subdominant for all scales that we are interested. For the Chaplygin gas,

$$+ AH - + BH^2 - \frac{3H^2}{2}(1 + w)_{ccc} = 0; \quad (12)$$

$$A = 1 - 6w(+1); \quad (13)$$

$$\begin{aligned}
 B = & - \frac{3H^2}{2}c_{ch} + 7 + c_{ch} + (13 - 3c_{ch}) + 6w^2 \\
 & 3c_{ch}(1 + 2w)^2 + \frac{2w}{3} - \frac{k^2}{H}; \quad (14)
 \end{aligned}$$

where the subscript  $c$  refers to cold dark matter.

For  $w = 0$ , (12) reduces to the expected, scale independent, CDM evolution with  $H \propto t^2$ . For  $w \neq 0$  we retain scale independence if  $w = 0$  and just get suppression of density perturbations in a similar fashion to a quintessence field. However for  $w \neq 0$  the perturbation evolution becomes scale dependent with the  $(k=H)^2$  term dominating the others for scales greater than a charac-

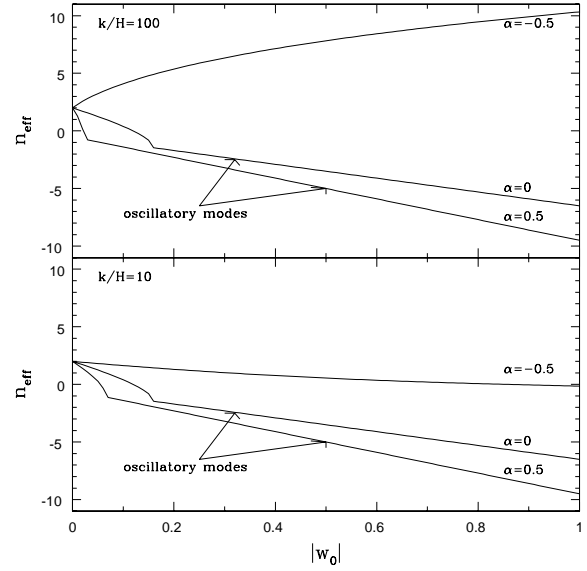


FIG. 3: Late time evolution envelope for  $n_{eff}$ . The power,  $n_{eff} = -\alpha$ , is plotted for two length scales  $k=H = 10$  and  $100$ . In the oscillatory regime  $n_{eff}$  for the bounding envelope is plotted.

teristic scale

$$k^2 = \frac{H^2}{jw_0j}; \quad (15)$$

There are 3 possible solution types, for  $k < k_c$ ,

$$\begin{aligned}
 [1] & : \text{growing mode; } < 0; \\
 [2] & : \text{decaying mode; } 0; \\
 [3] & : \text{oscillatory decay; } > 0;
 \end{aligned} \quad (16)$$

In figure 2 we show the asymptotic behavior at late times (taking  $w = jw_0j$ ) as one increases the scale  $k=H$ . In figure 3 we show the associated scaling of  $n_{eff}$ , plotting  $n_{eff} = -\alpha$ . For  $jw_0j \neq 0$ , and  $\alpha > 0 (< 0)$  GCG perturbations are suppressed (promoted) in comparison to those for a CDM model.

The GCG also has an effect on the CDM perturbations through the relation:

$$c + H \approx \frac{3H^2}{2} [c_{ccc} + (1 - 3w)c_{ch}] = 0; \quad (17)$$

If  $jw_0j \neq 0$  and  $\alpha > 0 (< 0)$  the GCG drives suppression (growth) in  $c$ . In figure 4 we show the power law evolution of  $c$ , plotting  $n_{eff;c} = -\alpha_c$  for 3 scales as one varies  $\alpha$ . The strong growth in  $c$  effectively rules out a GCG with  $\alpha < 0$  as a dark energy candidate.

Note that the  $\alpha = 0$  degeneracy present in the background evolution is not found in the perturbations. The matter power spectrum and CMB spectrum will therefore be better discriminators between  $\alpha$  and the GCG than SN 1a.

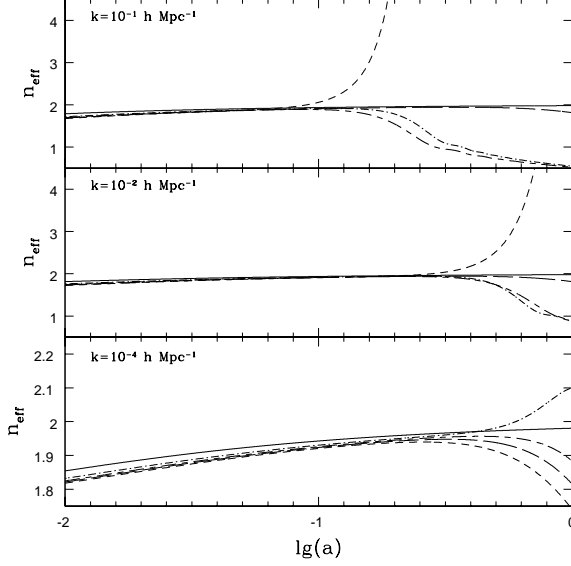


FIG. 4: Evolution of  $n_{\text{eff},c} = \frac{c}{a} = c$  for  $jw_0j = 0.5$  and  $= -0.1$  (short dash), 0 (long dash), 0.1 (long-short dash), 0.5 (dot dash) in comparison to pure CDM model (full line). Three length scales  $k = 10^{-4}; 10^{-2}; 10^{-1} \text{ hMpc}^{-1}$  are considered.

#### IV. IMPLICATIONS FOR TEMPERATURE ANISOTROPIES

A Chaplygin gas matter component would change the temperature anisotropy spectrum in a number of ways; altering the late-time ISW effect, the peak positions and relative heights.

The GCG's late-time evolution will alter the evolution of the gravitational potential the CMB photons pass through to reach us, inducing an ISW effect. Following [13] and again using the terminology of [12], the ISW temperature anisotropy is given by a source,

$$S_{\text{ISW}} = \frac{1}{a} \frac{d}{da} \left( \frac{3}{2} (1 + P) a^2 \right) - 3H a^2 (1 + P) \frac{1}{k^2} \quad (18)$$

where and are the Bardeen variables [14].

At late times the shear, , is negligible and it is the density perturbation that drives the ISW effect.

$$\frac{d}{da} \left( a^2 (1 + 3w) \frac{n_{\text{eff}}}{p} H \right) \quad (19)$$

where  $n_{\text{eff}}$  is the power law index and  $p = H$  as described in section III. Equation (19) shows why in a standard CDM scenario, with  $w = 0$  and  $n_{\text{eff}}$  and  $p$  both  $> 2$ , there is no appreciable ISW effect. In section III however we saw for  $w < 0$  that  $n_{\text{eff}} > 2$  giving a negative ISW effect, while for  $w > 0$ ,  $n_{\text{eff}} < 2$  producing an increase in the ISW temperature anisotropy. These effects are shown in figure 5.

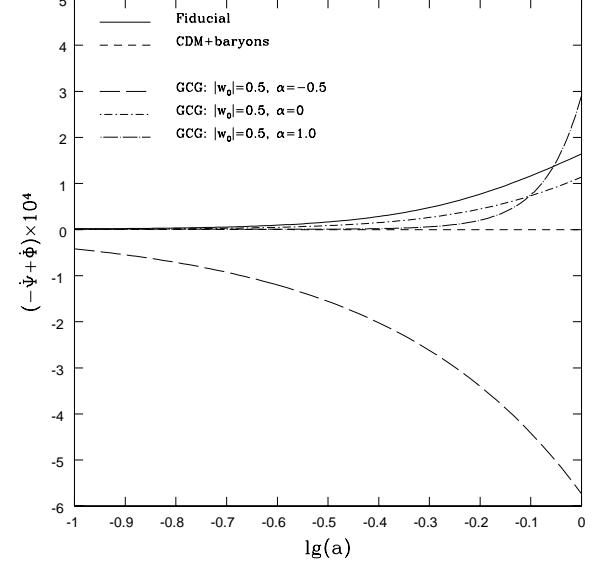


FIG. 5: Large scale ISW effect for GCG with  $= -0.5$  (long dash), 0 (short dash-dot) and 1 (long dash-dot) compared against a CDM + baryon (short dash) and 'fiducial'  $= 0.7; m = 0.3$  (full line) models.

The position of the first peak will be altered through adjustments to the sound horizon,  $r_{\text{shor}}$ , and angular diameter distance at the last scattering surface,  $d_A$ . The position of the first peak in multipole space is given by

$$l_A = \frac{d_A(z_{\text{rec}})}{r_{\text{shor}}(z_{\text{rec}})} \quad (20)$$

with

$$d_A = \frac{1}{H_0} \frac{Z_1^{\text{rec}}}{a_{\text{rec}}^0} \frac{1}{1 + \frac{1}{3} \frac{w_0 j}{a^{3(1+w)}}} \frac{1}{1 + \frac{1}{2} \frac{w_0 j}{a^{3(1+w)}}} \quad (21)$$

$$r_{\text{shor}} = \frac{1}{H_0} \frac{c_s^b d}{a_{\text{rec}}^0} \frac{1}{1 + \frac{1}{2} \frac{w_0 j}{a_{\text{rec}}^0}} \quad (22)$$

where  $a_{\text{rec}}^0$  is defined in equation (4) and  $c_s^b$  is the speed of sound for the radiation-baryon system, not to be confused with  $c_s$  for the Chaplygin gas (at this time the Chaplygin gas is behaving like dust and has  $c_s^2 = 0$ ). For fixed  $\lambda_b = \lambda_b h^2$  and  $\lambda_c = \lambda_c h^2$  ( $h = H_0 = 100$ ),  $l_A$  increases as one increases or as one decreases  $jw_0j$ . The position of the first peak would be the same for scenarios with the same value of  $\lambda_{\text{eff}}^0 d_A$ .

Because the Chaplygin gas matter at early times there is no simple degeneracy, governed by the peak positions, as there is for quintessence models (see

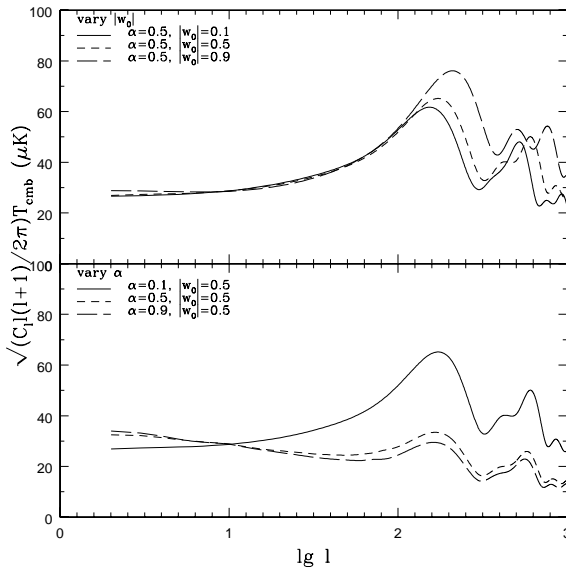


FIG. 6: Comparison of CMB power spectra, normalized to COBE at  $l = 10$ , with varying  $w_0$  and  $j_0$  keeping all other relevant quantities fixed. The behavior of peak heights and positions is discussed in the text.

for example [15]). The peak heights, when compared to the low  $l$  ‘plateau’, depend upon  $w_0$  and  $j_0$  through their influence on the ISW effect, the horizon scale at matter-radiation equality,  $l_{eq}$ , (through  $\frac{0}{m_{eff}}h^2$ ) and the depth of the potential well at last scattering (also through  $\frac{0}{m_{eff}}h^2$ ).

We follow the phenomenological discussion in [16], to predict how the peak heights will alter for fixed  $\Omega_b$  and  $\Omega_c$ . Increasing  $w_0$  increases  $\frac{0}{m_{eff}}$ , so that matter-radiation equality happens earlier, increasing  $l_{eq}$  and curtailing the driving effect that the decay of the gravitational potential has on oscillations during the radiation era. This lowers the height of the first peak, a decrease which is compounded by the raising of the plateau from the ISW effect. An earlier matter-radiation equality also decreases the depth of the potential well at last scattering, which combined with the reduction in radiation driving, increases the height of the third peak in comparison to the first and second ones.

As one increases  $j_0$  one decreases  $\frac{0}{m_{eff}}$ , lowering  $l_{eq}$ , and increasing the height of the first peak. This is tempered, however, by the increase in plateau height from the ISW effect. Reducing  $l_{eq}$  acts to decrease the height of the third peak in comparison to the second and first ones. These behaviors are confirmed by the full analysis, as is shown in figure 6.

The multitudinous effects that the GCG has on the CMB spectrum make comparison with CMB observations a strong test for the GCG models as will be seen below.

## V. CHAPLYGIN GAS LIKELIHOOD ANALYSIS

In order now to assess the viability of a GCG + CDM + baryon universe, we turn to evaluate the probability (the posterior) of these models given some current observations, namely SN 1a, CMB and LSS probed through galaxy survey.

To study the posterior distribution, we use the Baye’s theorem and rewrite it as the product of the likelihood and the prior (we assume the evidence is constant and thus ignore it). To probe this posterior, we consequently compute both the likelihood and the prior at various positions in the chosen restricted parameter space. This sampling is conducted via the construction of a Monte Carlo Markov Chain through the Metropolis-Hastings algorithm. Once converged, this chain provides us with a collection of independent samples from the posterior (see [17, 18, 19] for an introduction to this technique in this context and [20, 21] for general guidance).

Our code uses some likelihood computations elements from the code described in [19], and relies on a version of the CMB code [22] extended to include a Chaplygin gas component in order to calculate CMB power spectra and matter power spectra. As input data, we considered the apparent magnitudes of 51 Supernovae [2], CMB data sets from COBE [23], MAXIMA [24], BOOMERANG [25], and VSA [26] and large scale structure data from 2dF [27]. We consider only models, i.e.  $\kappa = 0$  with scale invariant initial power spectrum, i.e.  $n_s = 1$ . We use stringent (Gaussian) priors on  $H_0$  using the HST Key Project results  $h = 0.72 \pm 0.08$  [28] and on  $\Omega_b = \Omega_b h^2 = 0.02 \pm 0.001$  using BBN constraints [29].

We normalize the matter power spectrum using  $A_s$ , the initial power spectrum normalization, and following [30], we use  $a$  and  $b_1$  to parameterize redshift-space distortions and (linear) bias respectively. The power spectrum is then related to the transfer function  $T(k)$  (computed with CAMB) by

$$P(k) = A_s \left(1 + \frac{2}{3} + \frac{2}{5} b_1^2 T(k)^2\right) \quad (23)$$

In order to alleviate the natural degeneracy between  $A_s$  and  $b_1$  (as far as LSS constraints are concerned), we use the 2dF results [31, 32] to impose strong (Gaussian) priors on  $a$  and  $b_1$ , i.e.  $a = 0.54 \pm 0.09$ ;  $b_1 = 1.04 \pm 0.11$ .

Throughout this analysis, we ensured the chains’ convergence by generating and comparing several of them (typically containing  $10^5$  elements) and by checking the so-called ‘parameter mixing’ among them. After several trials, we choose the proposal density for each parameter to be a Gaussian whose width is close to the final one and whose center is the last chain values. This allows a full exploration of the parameter space. To pick-up the next chain element, we allow only 1 to 3 directions (this number is randomly chosen) to vary. This gives us an acceptance rate around 25%, a good target value for efficiency’s sake [20]. The first 4000 elements of the chain,

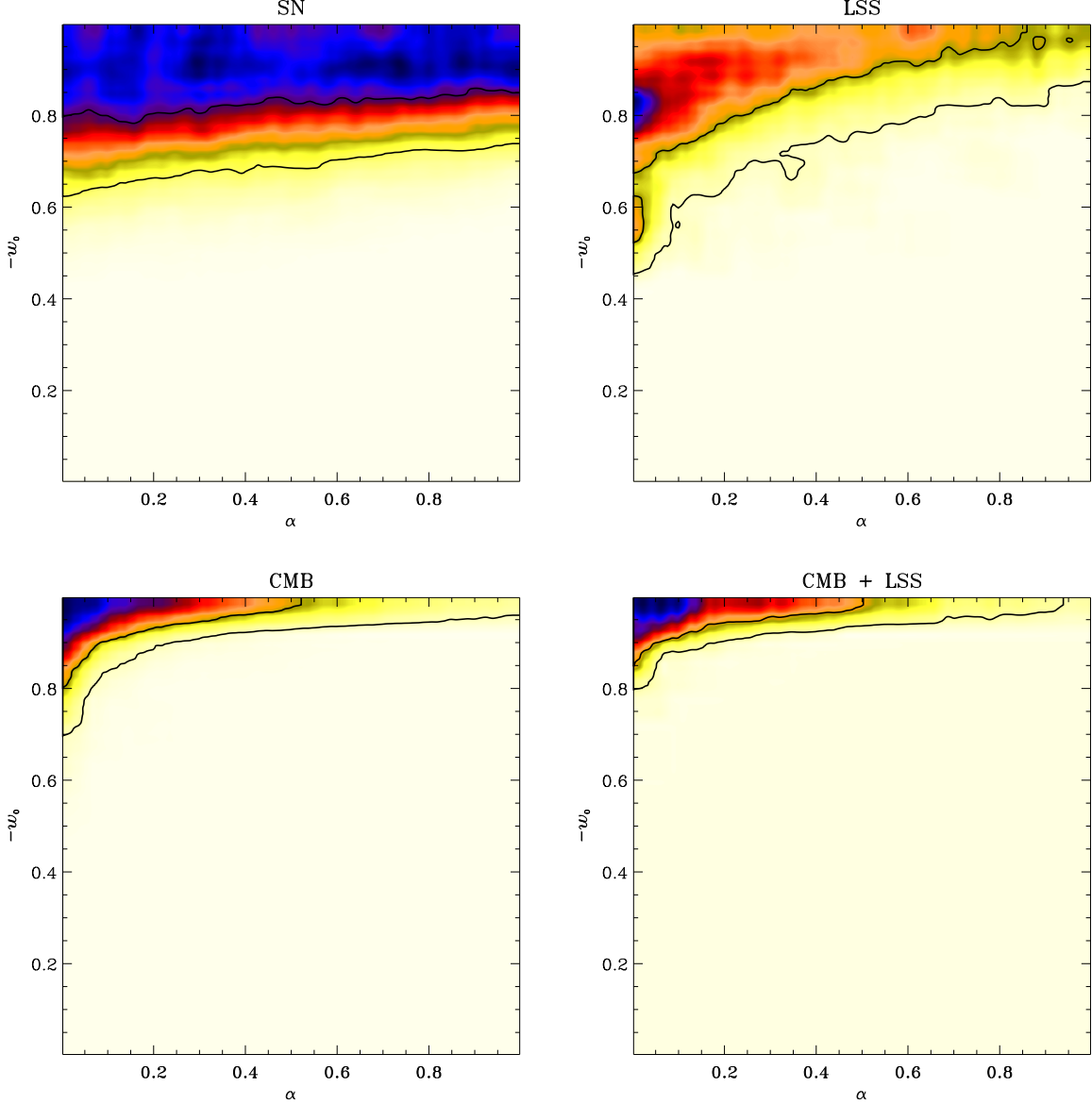


FIG. 7: Joint posterior of the  $\alpha$  and  $-w_0$  parameters considering only SN 1a data (top-left panel), LSS data (top-right panel), CMB data (bottom-left) and jointly CMB and LSS data (bottom-right). The contours represent the subsequent 68% and 95% confidence regions. While SN 1a data induce constraints that are quite loose, LSS and CMB constraints are much tighter and tend to favor a cosmological constant like scenario.

prior to its convergence, are thrown away and no extra thinning is applied [20].

Once converged, the chains provide a fair sampling of the full posterior distribution so that we can deduce easily from it all the quantities of interest, e.g. the (joint) marginalized distribution of any parameter(s).

As stated above, we are interested in finding the compatibility of a Chaplygin gas + CDM + baryon universe with current data. For this we vary only 8 parameters  $\{h, \Omega_b, \Omega_{cdm}, w_0, b, A_s, n_s, \tau\}$  and impose the priors stated above. Following section III's discussion, we restrict ourselves to  $0 < h < 1$  and  $0 < w_0 < 1$ . In figure 7 we plot

the marginalized joint distribution of the  $\alpha, w_0$  parameters (which is in this case just the joint number density of those parameters), as well as the 68% and 95% confidence contours, considering separately SN 1a, LSS, CMB data sets, and also jointly CMB and LSS. Note that for visual purposes only the displayed surface has been built by oversampling our samples using cubic interpolation. This does not affect the quantitative interpretation since the distributions turn out to be smooth.

The interpretation of the contours is nicely consistent with the theoretical prospects discussed above. First, the SN 1a observations (top-left panel) offer very light con-

straints on the GCG parameters, since they are sensitive only to the background evolution. Any value appears viable, extending thus the obvious degeneracy between  $\Lambda$ -CDM models and GCG models with  $w = 0$  discussed in section II (e.g. see figure 1). As soon as density perturbations are considered, the constraints tighten drastically. For both LSS and CMB, the isocontours are roughly centered on the  $w = 0, w_0 = -1$  model, that corresponds to the GCG acting like a term. This fact is emphasized in the joint CMB + LSS analysis. Note that in the limit that  $w_0$  tends to  $-1$  (we however impose  $w_0 < 1$ ), the GCG component tends to behave like a term, irrespective of the precise value of  $w$ , thus leading to the observed degeneracy in the  $w_0 = -1$  direction.

The other varied parameters, i.e.  $h$ ,  $\Omega_b$  and  $\Omega_{\text{CDM}}$ , as well as the atness imposed on  $h$ , exhibit (joint) distributions similar to those found in typical  $\Lambda$ -CDM model studies (see e.g. [19]). This leads us to the the main conclusion of this study: the current data tends to favor ordinary theory. When marginalized over all other parameters, we indeed find,  $< 0.5; 0.93$ , and  $w_0 < -0.85; -0.8$ , both respectively at the 68% and 95% confidence level.

## V I. CONCLUSIONS

We have investigated the effect of a Chaplygin gas matter component in the universe's ingredients, to see if such a component is consistent with observations and whether

it is a feasible alternative to  $\Lambda$ .

Through inherent degeneracies with  $\Lambda$  in the background evolution, the Chaplygin gas models have a good fit with SN 1a data. These degeneracies are not present, however, in the perturbation evolution. In particular the growth/suppression of both GCG and CDM density perturbations for  $w \neq 0$  proves distinctive when comparing against large scale structure observations. The GCG also introduces a number of distinguishing differences from the  $\Lambda$ -CDM CMB spectrum through altering the potential at last scattering, the ISW signature, the equality scale, and the angular diameter distance to last scattering. Combined, these differences provide a strong test for the GCG scenario.

We performed likelihood analyses using SN 1a, CMB and LSS datasets and found that the current data strongly prefers a  $\Lambda$ -like matter component, with  $w < 0.5$  and  $w < -0.85$  at the 68% level. Consequently, on the basis of current observations, Chaplygin gases do not seem to provide a favored alternative to scenarios involving a cosmological constant.

Acknowledgments We would like to thank Elena Pierpaoli, David Spergel, and Licia Verde for very helpful discussions in the course of this work. RB and OD are supported by MAP and NASA ATP grant NAG 5-7154 respectively.

---

[1] P. M. Garnavich et al, *Astrophys. J. Lett.* 493, L53-57 (1998); S. Perlmutter et al (The Supernova Cosmology Project), *Nature* 391 51 (1998); A. G. Riess et al, *Astrophys. J.* 116 1009 (1998); B. P. Schmidt, *Astrophys. J.* 507 46-63 (1998).

[2] S. Perlmutter et al, *Astrophys. J.* 483, 565 (1997) 391 51 (1998); A. G. Riess et al, *Astrophys. J.* 116 1009 (1998); B. P. Schmidt, *Astrophys. J.* 507 46-63 (1998).

[3] P. J. E. Peebles, B. Ratra, *RMP* (2003) in press, [astro-ph/0207347](http://arxiv.org/abs/astro-ph/0207347).

[4] H. Sandvik, M. Zaldarriaga, I. Waga, [astro-ph/0212144](http://arxiv.org/abs/astro-ph/0212144).

[5] A. Yu. Kamenshchik, U. M. Moschella, V. Pasquier, *Phys. Lett. B* 511 265 (2001).

[6] N. Bilić, G. B. Tupper, R. D. Viollier, [astro-ph/0111325](http://arxiv.org/abs/astro-ph/0111325).

[7] M. C. Bento, O. Bertolami, A. A. Sen, *Phys. Rev. D* 66 043507 (2002), [astro-ph/0202064](http://arxiv.org/abs/astro-ph/0202064); [astro-ph/0210375](http://arxiv.org/abs/astro-ph/0210375).

[8] J. C. Fabris, S. V. B. G.oncalves, P. E. deSouza Gen. Rel. Grav. 34 2111 (2002), [astro-ph/0203441](http://arxiv.org/abs/astro-ph/0203441); Gen. Rel. Grav. 34 53 (2002), [astro-ph/0103083](http://arxiv.org/abs/astro-ph/0103083); [astro-ph/0207430](http://arxiv.org/abs/astro-ph/0207430).

[9] P. F. Gonzalez-Diaz, [astro-ph/0221414](http://arxiv.org/abs/astro-ph/0221414).

[10] C. De Ayet, S. Landau, J. Raux, M. Zaldarriaga, P. A. Stier, *Phys. Rev. D* 66 024019 (2002), [astro-ph/0201164](http://arxiv.org/abs/astro-ph/0201164).

[11] D. P. O' Dolsky, *Astrophys. J.* 28 434 (2002), [gr-qc/0203010](http://arxiv.org/abs/gr-qc/0203010).

[12] E. Bertschinger, C.-P. Ma, *Astrophys. J.* 457 5 (1995), [astro-ph/9506072](http://arxiv.org/abs/astro-ph/9506072).

[13] U. Seljak, M. Zaldarriaga *Astrophys. J.* 469 437 (1996), [astro-ph/0006436](http://arxiv.org/abs/astro-ph/0006436).

[14] J. M. Bardeen *Phys. Rev. D*, 22 1882 (1980).

[15] R. Bean, A. Melchiorri *Phys. Rev. D* 65 041302 (2002), [astro-ph/0110472](http://arxiv.org/abs/astro-ph/0110472).

[16] W. Hu, M. Fukugita, M. Zaldarriaga, M. Tegmark *Astrophys. J.* 549 669 (2001).

[17] N. Christensen, R. M. Eyer, [astro-ph/0006401](http://arxiv.org/abs/astro-ph/0006401).

[18] N. Christensen, R. M. Eyer, L. Knox, B. Luey, *Classical and Quantum Gravity* 18 2677 (2001), [astro-ph/0103134](http://arxiv.org/abs/astro-ph/0103134).

[19] A. Lewis, S. Bridle, [astro-ph/0205436](http://arxiv.org/abs/astro-ph/0205436).

[20] Eds W. R. Gilks, S. Richardson, D. J. Spiegelhalter, *Markov Chain in Practice*, Chapman & Hall, 1996.

[21] S. Chib & E. G. Greenberg, *The American Statistician* 49 4 (1995).

[22] A. Lewis, A. Challinor, A. Lasenby, *Astrophys. J.* 538 473 (2000).

[23] G. Smoot et al, *Astrophys. J.* 386 L1 (1992), C. Bennett et al *Astrophys. J.* 464 L1 (1996).

[24] S. Hanany et al, *Astrophys. J. Lett.* 545 L5 (2000), [astro-ph/0005123](http://arxiv.org/abs/astro-ph/0005123).

[25] C. B. Netterfield et al, *Astrophys. J.* 571 604 (2002), [astro-ph/0104460](http://arxiv.org/abs/astro-ph/0104460).

[26] P. F. Scott et al, [astro-ph/0205380](http://arxiv.org/abs/astro-ph/0205380).

[27] O. Lahav et al, *MNRAS* 333 961L (2002), [astro-ph/0112162](http://arxiv.org/abs/astro-ph/0112162).

[28] W. L. Freedman et al, *Astrophys. J.* 553 47 (2001), [astro-ph/0012376](http://arxiv.org/abs/astro-ph/0012376).

[29] S. Burles, K M . Nollett, & M . S. Turner, *A strophys. J.* 552 L1 (2001), astro-ph/0010171.  
 [30] A J.S. Hamilton, *A strophys. J.* 385,15 (1992).  
 [31] J.A . Peakcock et al., *Nature* 401 169, astro-ph/0103143.  
 [32] L.Verde et al., *M N R A S* 335 432, astro-ph/0112161.

## V II. APPENDIX - PERTURBATION E VOLUTION FOR A C H A P L Y G IN G A S

We use the basic background equation (time derivatives with respect to  $t$ ):

$$\dot{H} + H^2 = \frac{\dot{a}}{a} = \frac{H^2}{2} - 1 - 3 \sum_i (w_i) \quad (24)$$

and equation of state and speed of sound equations:

$$c_s^2 = \frac{P}{\rho} = \frac{P}{\rho} \quad (\text{assuming adiabaticity}) \quad (25)$$

! !

$$w = - \frac{P}{\rho} = 3H(1+w)(c_s^2 - w) \quad (26)$$

Following [12] the first order perturbation equations are

$$\dot{h} = (1+w) + \frac{h}{2} - 3c_s^2 w H \quad (27)$$

$$\dot{h} = 1 - 3c_s^2 H + \frac{c_s^2}{(1+w)} k^2 : \quad (28)$$

So that the second order equation in (differentiating (9)) is given by

$$\dot{h} = (1+w) - \frac{h}{2} - w - \frac{h}{2} - 3c_s^2 w (H + h) \rightarrow 3c_s^2 w H : \quad (29)$$

We eliminate the time derivatives of the metric perturbation,  $h$ , using the perturbed Einstein equations

$$k^2 - \frac{1}{2} H h = - \frac{1}{2} a^2 \quad (30)$$

$$h + 2H - 2k^2 = 3a^2 P \quad (31)$$

which give

$$(1+w) \frac{h}{2} = H - + (1+w)H + 3(c_s^2 - w)H^2 - (1+w) \frac{a^2}{2} (+ 3P) : \quad (32)$$

Collecting terms together we obtain the general evolution equation for for any uid with equation of state  $w$  and speed of sound  $c_s$ ,

$$= 3c_s^2 (1+w)H - [1 + 6(c_s^2 - w)]H - c_s^2 k^2 + 9(c_s^2 - w)^2 H^2 + 3c_s^2 w H + 3 \frac{a}{a} (c_s^2 - w) + (1+w) \frac{a^2}{2} (+ 3P) : \quad (33)$$

Specializing to the Chaplyin gas in the matter dominated era

$$\frac{a^2}{2} (+ 3P) = \frac{3H^2}{2} - c_{ch} (1 + 3c_s^2) + c_c \quad (34)$$

$$\frac{a}{a} = \frac{H^2}{2} (1 - 3c_{ch}w) \quad (35)$$

$$c_s^2 = w \quad (36)$$

$$c_s^2 = 3Hw(1+w)(1+w) \quad (37)$$

we find

$$+ [1 - 6w(+1)]H - wk^2 + \frac{3H^2}{2} f_{ch} + (7 + c_{ch}) + (13 - 3c_{ch}) + 6w^2 w - 3c_{ch}(1+2)w^2 = \frac{3H^2}{2}(1+w)c_c + 3w(1+w)H : \quad (38)$$

Similarly if one applies equation (33) to CDM with  $w = c_s^2 = 0$ , we find

$$c_c + H = \frac{3H^2}{2} [c_c + (1 - 3w)c_{ch}] = 0 : \quad (39)$$